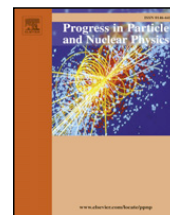


Contents lists available at [ScienceDirect](http://www.sciencedirect.com)

Progress in Particle and Nuclear Physics

journal homepage: www.elsevier.com/locate/ppnp

Review

Modeling nuclear dynamics and weak interaction rates during the supernova collapse phase

Terrance Strother, Wolfgang Bauer*

Department of Physics and Astronomy and National Superconducting Cyclotron Laboratory, Michigan State University, East Lansing, MI 48824, USA

ARTICLE INFO

Keywords:
Supernova
Heavy ion
Transport theory

ABSTRACT

Motivated by the success of kinetic theory in the description of observables in intermediate and high energy heavy ion collisions, we use kinetic theory to model the dynamics of the early stage of a type II core collapse supernova. The algorithms employed to model the collapse, the rationale for choosing them, and the results of this preliminary calculation are discussed. The main innovation in the present calculation is to introduce a coupled channel weak interaction reaction network of heavy nuclei, which supersedes the conventionally used approximation of a representative heavy nucleus used in neutrino Boltzmann transport.

© 2009 Elsevier B.V. All rights reserved.

1. Introduction

Transport theories based on a semiclassical implementation of kinetic theory [1–7] have been quite successful at modeling intermediate and high energy nuclear collisions. Given the numerous similarities between requirements that simulations of nuclear collisions and supernovae [8–14] must satisfy, such as the ability to model particle production, shock wave formation, collective deflection, as well as the interplay between regular and chaotic collective dynamics, it is tempting to implement these types of kinetic theory based approaches to model the physics and astrophysics of supernova explosions. This is the aim of our work.

To solve the relevant transport equations [15], we use the test particle method [16], where phase space distribution functions are represented by sums over delta functions. The initial coordinates of these delta-function point particles (test particles) are chosen to be consistent with the initial conditions core being modeled. With this approach, we can derive first order differential equations for the centroid coordinates of these test particles.

As discussed in our previous work [17], our code is designed to run on large multi-processor installations and is capable of calculating all desired statistical distributions in the full three-dimensional space and propagating test particles in the full six-dimensional phase space. However, for debugging purposes, we also want to provide ways to test the implementation of our ideas on a single processor. The calculation discussed here is performed exactly for that purpose and is a simulation of early stages of the collapse of a non-rotating spherically symmetric core [18]. While test particles are still propagated in the full six-dimensional phase space, due to statistical limitations imposed by working on a single processor [17], we assume that all statistical distributions are spherically symmetric. The algorithms employed to calculate the spherically symmetric statistical distributions are discussed in detail in our previous work [17].

2. Test particle properties

Matter and neutrino test particles are used to model the core. Matter test particles are assumed to be electrically neutral and have nuclear properties that are initially chosen to be consistent with the chemical composition of the progenitor [18]. At

* Corresponding author. Tel.: +1 517 353 8662; fax: +1 517 353 4500.
E-mail address: bauer@pa.msu.edu (W. Bauer).

later times, these nuclear properties are determined by local electron capture rates and the number and type of interactions each matter test particle has with neutrino test particles. The centroid of each matter test particle is subject to three forces: gravitation, a mean field nuclear force, and a force exerted by the surrounding electron gas on the electrons it implicitly represents. The latter two forces are lumped together and denoted by $-\vec{\nabla}U_{EoS}$. Matter test particles can scatter with one another and with neutrino test particles. The equations of motion for the centroid coordinates of the matter test particles are given by

$$\frac{d}{dt}\vec{p}_j = \vec{F}_{G,j} - \vec{\nabla}U_{EoS}(\vec{r}_j) + \vec{C}(\vec{p}_j) \quad (1)$$

$$\frac{d}{dt}\vec{r}_j = \frac{\vec{p}_j}{\sqrt{m^2 + p_j^2}} \quad (2)$$

$$j = 1, \dots, N,$$

where $\vec{C}(\vec{p}_j)$ symbolizes the effects that two-body collisions with other matter and neutrino test particles have on the j th matter test particle's momentum. N is the number of matter test particles used to model the core. For calculations to be able to run on a single processor, N cannot greatly exceed 10^6 , otherwise run times become prohibitively long [17].

Neutrino test particles oscillate between electron and muon states. Neutrino test particles of both species are assumed to be massless, move at the speed of light, and subject to no forces due to mean field potential. The only way they can interact with other test particles is through scattering with or being captured by matter test particles, where the latter channel is available only to electron neutrino test particles. Thus the propagation of neutrino test particles between interactions with matter test particles is quite simple.

3. Statistical distributions

To calculate the spherical statistical distributions, we define a set of concentric spherical shells with radii chosen such that each shell contains a fixed number of matter test particles. We then use the test particles in each shell to compute the statistical quantities of interest, density, electron fraction, nuclear composition, temperature, etc. at its average radius and store them so that these quantities can be linearly interpolated at arbitrary radii. To minimize the effects of statistical fluctuations on the calculations of statistical distributions and their radial derivatives, there must be a lower limit imposed on the number of matter test particles contained in each shell. Thus for a fixed number of matter test particles N , there is a maximum number data points at which the statistical distributions and their radial derivatives can be known. For single processor calculations with N being of the order of 10^6 , the maximum number of data points that can be generated is approximately 100. With this low number of data points spread over the entire radius of the core, we can only trust the interpolation of statistical quantities and their derivatives during two stages of the collapse. We can safely linearly interpolate at arbitrary points in the early stage of the collapse, before the statistical distributions start radially changing too rapidly, and in the late stages of the collapse, after the core has contracted significantly allowing data points to be generated sufficiently close to one another to resolve rapid radial changes. The intermediate stages of the collapse cannot be modeled with 100 data points and it is for this reason that we limit this preliminary test calculation to the early stage of the collapse.

4. Matter test particle interactions

In the early stage of the collapse, it is sufficient to treat gravitation with Newtonian mechanics. Working in this limit with the assumption of spherical symmetry makes our modified Newtonian monopole model, discussed in detail in our previous work [19], an ideal solution. To calculate the force a matter test particle feels from the electron gas, we calculate the quantum statistical interaction potential energy of the electrons it implicitly represents and the electron gas surrounding its centroid U_{QSI} . We then take the force exerted by the electron gas to be $-\vec{\nabla}U_{QSI}$. To calculate U_{QSI} , we assume that the electron gas is ideal and degenerate. The latter assumption is valid in the early stage of the collapse as it is not until later in the collapse that electron up-scattering off neutrinos lifts the degeneracy condition and finite temperature corrections must be taken into account [20]. The nuclear force is largely negligible in the early stage of the collapse as the density is everywhere well below nuclear matter density. However, for completeness, we include it in this calculation and it is taken to be $-\vec{\nabla}U_{nuc}$, where U_{nuc} is the nuclear equation of state mean field potential. Here we approximate the nuclear mean field potential with a simple density dependent functional. It should be noted that simulations of full collapses will include more complicated electron gas and nuclear forces that are temperature dependent. Furthermore, momentum dependent isospin potentials [21, 22] can sensibly be included as we have full knowledge of the nuclear composition everywhere in the core. In addition to the forces that matter test particles directly and indirectly exert on one another, they can scatter off other nearby matter and neutrino test particles. The way we model test particle scattering is explained at length in our previous work [17]. Here it suffices to say that test particle scatterings are modeled relativistically in a way similar to those used in the simulation of heavy ion collisions [23].

5. Weak interactions

Weak interactions are modeled two different ways in our simulation. Neutrino production is modeled by accessing rate tables and neutrino-matter interactions are modeled by explicitly propagating neutrino test particles. Each time a neutrino test particle is created or captured in a spherical shell, the nuclear properties of a matter test particle in that shell are updated in a way that is consistent with the type of weak test particle interaction that occurred. A simple electron or neutrino capture requires decreasing or increasing the nuclear charge of the nuclei represented by the capturing matter test particle. A complex electron or neutrino capture requires accessing nucleon emission channels that increase the free baryon to nucleus ratio of the capturing matter test particle and changing the type of nucleus it represents. Complex weak reactions are used to ensure the final state of the nuclei represented by the capturing matter test particle are included in the table of nuclei used in our simulation and can also be activated when the nucleus-lepton relative energies become sufficiently high. The algorithm used to accomplish this is discussed in detail in our previous work [17]. In this way we model the propagation of an ensemble of nuclei and have full knowledge of the nuclear composition of each spherical shell. Given that most supernova simulations only track the abundances of free baryons, alpha particles, and an average “heavy” nucleus, this is a significant advantage that our approach offers. Nuclear structure effects massively impact the deleptonization rate [20,24], and many of these effects can be missed if one speaks of an average “heavy” nucleus instead of an ensemble of nuclei. Furthermore, explicit knowledge of nuclear composition may lead to a better understanding of the propagation of the shock wave. This is so as the dissociation of heavy nuclei a key process for shock wave energy loss [20] and structure effects can influence the susceptibility of a given nucleus to dissociation.

5.1. Neutrino production

Currently, we only model the production of neutrinos by electron capture in the early stage of the collapse. Other mechanisms of neutrino production occur [24], however these are strongly temperature dependent [24,25] and unimportant until the late stage of the collapse and/or they involve excited nuclear states and are poorly understood. Since we do not explicitly model the propagation of electron test particles, we use electron capture rate tables to model neutrino production. Knowing the density, electron fraction, and temperature in each spherical shell, we can access the electron capture rate for all the nuclear species present in a given shell. The number of neutrino test particles created by electron capture by a given nuclear species present in a shell is then determined with a Monte Carlo algorithm. Newly created neutrino test particles' energies are determined by the local electron momentum distribution and their momentum vectors are oriented randomly.

5.2. Neutrino-matter interactions

Neutrino-matter interaction cross sections are far too small to directly simulate weak reactions during matter-neutrino test particle collisions. The number of events required to have even a few weak test particle interactions occur per time step during test particle pair scatterings is prohibitively large. Instead we use simple mean free path formulas and a Monte Carlo algorithm to decide if a neutrino test particle will interact with matter test particles in the spherical shell containing it. If it is determined that an interaction occurs, the relevant matter-neutrino interaction cross sections [25] are used to generate relative probabilities of interaction and a Monte Carlo algorithm is used to select an interaction channel. If a capture channel is selected, it is modeled in the way described above. If an elastic channel is selected, the neutrino test particle is elastically scattered off of a nearby matter test particle. As previously mentioned, neutrino test particles propagate freely between interactions. The ability of our approach to simultaneously solve of the matter and neutrino transport problem in the full six-dimensional phase space is arguably the greatest advantage it offers.

6. Coupled channel weak interaction reaction network

The purpose of the present study is to implement the propagation of an ensemble of nuclear isotopes in a coupled channel weak reaction network, which is in contrast to the current state of the art for neutrino Boltzmann transport, which has to rely on the approximation of propagating a single representative species of heavy nucleus. We have tested our implementation in a simple case that can be run on a single processor. Matter test particle angular momentum and energy were conserved well during the early stage of the collapse. Not until the intermediate stage of the collapse started and knowledge of the density and its radial derivative became unreliable did fictitious forces, particularly in the lower density region of the core, start to cause violations in energy conservation and unphysical test particle motion. As previously stated, this problem is expected to disappear when the number of test particles becomes sufficiently high. Qualitative expectations such as an initially slow but eventually rapid decrease of the electron fraction in the inner core, leading to a rapid inward acceleration of the matter in there, the majority of the neutrinos test particles produced escaping the core, etc. were met as well. A snapshot of the nuclear composition of the core at what we define to be the end of the early stage of the collapse is included in Fig. 1.

Initially, the core is assumed to be made of ^{54}Fe , ^{56}Fe , and smaller admixtures of Fe-like nuclei with atomic mass numbers in the range [45, 65] and neutron excesses greater than ^{56}Fe . After 0.08 s, not only are there many nuclei with neutron excesses much larger than ^{56}Fe that have captured one or more electrons, there are also some nuclei with lower neutron

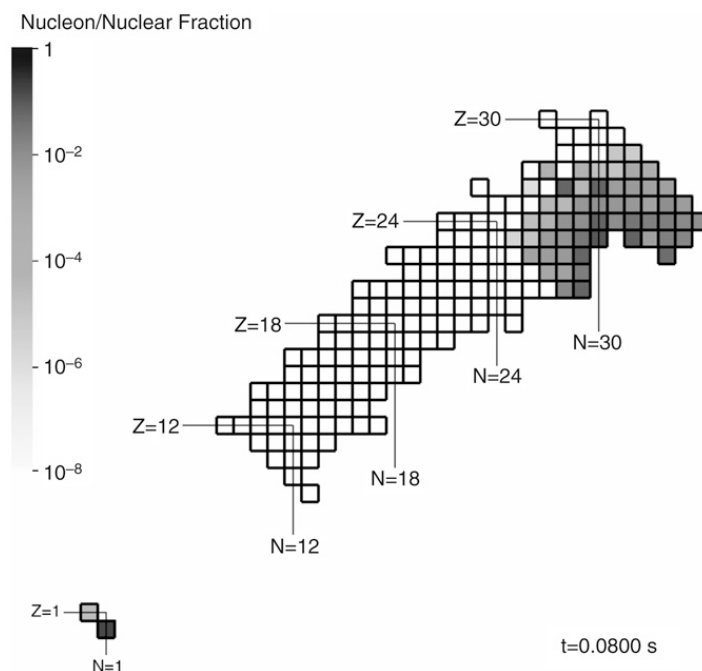


Fig. 1. Nuclear composition of the core at $t = 0.08$ s.

excesses than ^{54}Fe that have evidently captured one or more neutrinos. Furthermore, free baryons are now present in the core. In fact, roughly ten percent of all free baryons and nuclei in the core are free neutrons at this point.

7. Summary and prospects

This simulation is a work in progress. We are encouraged that our coupled channel algorithms for the simultaneous propagation of an ensemble of isotopes instead of the conventional one-heavy-nucleus approximation are functioning as expected at the single processor level. When full three dimensional simulations that follow the collapse through bounce are run, we expect to see the deviations from spherical symmetry in the density distribution that we both intuitively expect, due to angular momentum conservation, and have seen in previous preliminary calculations [19]. We hypothesize that the density depletion along the axis of rotation will lead to focussing of neutrino emission along the poles which will amplify the parity violation induced recoil kick scenario proposed for the neutron star remnant by Horowitz et al. [26,27]. However, before we can reach quantitative conclusions to substantiate this claim, we must port our algorithms to a highly parallelized multi-processor facility.

Acknowledgments

This research was supported by the US National Science Foundation under grants PHY-0245009 and PHY-0555893, and an Alexander-von-Humboldt Foundation Distinguished Senior US Scientist Award.

References

- [1] G.F. Bertsch, Phys. Rev. C 29 (1984) 673.
- [2] H. Kruse, Phys. Rev. Lett. 54 (1985) 289.
- [3] W. Bauer, G.F. Bertsch, W. Gassing, U. Mosel, Phys. Rev. C 34 (1986) 2127.
- [4] H. Stöcker, W. Greiner, Phys. Rep. 137 (1986) 277.
- [5] G.F. Bertsch, S. Das Gupta, Phys. Rep. 160 (1988) 189.
- [6] P. Schuck, Prog. Part. Nuclear Phys. 22 (1989) 181.
- [7] W.G. Gong, W. Bauer, C.K. Gelbke, S. Pratt, Phys. Rev. C 43 (1991) 781.
- [8] J.R. Wilson, Numerical Astrophysics, Jones and Bartlett, Boston, 1985.
- [9] M. Herant, W. Benz, W.R. Hix, C.L. Fryer, S.A. Colgate, Astrophys. J. 435 (1994) 339.
- [10] C.L. Fryer, A. Heger, Astrophys. J. 541 (2000) 1033.
- [11] R. Buras, M. Rampp, H.-Th. Janka, K. Kifonidis, Phys. Rev. Lett. 90 (2003) 241101.
- [12] H.-Th. Janka, R. Buras, M. Rampp, Nuclear Phys. A 718 (2003) 269c.
- [13] A. Mezzacappa, M. Liebendörfer, O.E.B. Messer, W.R. Hix, F.-K. Thielemann, S.W. Bruenn, Phys. Rev. Lett. 86 (2001) 1935.
- [14] T.A. Thompson, A. Burrows, P.A. Pinto, Astrophys. J. 592 (2003) 434.
- [15] W. Bauer, Acta Phys. Hung. A 21 (2004) 371.
- [16] C.-Y. Wong, Phys. Rev. C 25 (1982) 1460.
- [17] T. Strother, W. Bauer, Int. J. Modern. Phys. D (2008) (submitted for publication).
- [18] S.E. Woosley, T.E. Weaver, Ann. Rev. Astron. Astrophys. 24 (1986) 205.

- [19] W. Bauer, T. Strother, *Int. J. Mod. Phys. E* 14 (2005) 129.
- [20] G. Matrínez, M. Liebendörfer, D. Frekers, *Nuclear Phys. A* (2004).
- [21] B. Li, C.B. Das, S.D. Gupta, C. Gale, *Nuclear Phys. A* (2004).
- [22] B. Li, L. Chen, C.M. Ko, *Phys. Rep.* 464 (2008) 113–281.
- [23] G. Kortemeyer, F. Daffin, W. Bauer, *Phys. Lett. B* 374 (1996) 25.
- [24] G. Matrínez, *Eur. Phys. J* (2005).
- [25] A. Burrows, T. Thompson, *Astrophys. J.* (2002).
- [26] C.J. Horowitz, Gang Li, *Phys. Rev. Lett.* 80 (1998) 3694.
- [27] C.J. Horowitz, J. Piekarewicz, *Nuclear Phys. A* 640 (1998) 281.